THE KARLSRUHE PULSED SUPERCONDUCTING MAGNET PROGRAMME

Status Report[+]

The Karlsruhe IEKP Magnet Group; compiled by W. Schauer
Institut für Experimentelle Kernphysik, Gesellschaft für Kernforschung, Karlsruhe, Germany

Abstract

This paper reviews the progress of the Karlsruhe superconducting pulsed magnet work. The experimental results of the first two magnets are discussed and the present status of the subsequent magnet family D2a, D2b and D3 is described. Results of superconductor and material properties measurements are presented.

I. Introduction

The high magnetic field capabilities of superconducting materials make possible the construction of pulsed accelerator magnets which are especially suitable for large synchrotrons with low repetition rates. With the construction of the 300 GeV proton accelerator now under way at CERN, the application of high field pulsed superconducting magnets to increase the present machine energy to about 1000 GeV has been taken into consideration. Convincing demonstrations must show their suitability and reliability before a decision can be made whether superconducting pulsed magnets should be adopted to uprate the machine energy. Each group of the GESSS Collaboration, comprising the development teams at Rutherford Laboratory, CEN/Saclay and IEKP Karlsruhe, has built and is going to build and test several different prototype magnets which will be in line with the requirements of a superconducting accelerator concept. - This paper gives the Karlsruhe laboratory status report with respect to pulsed superconducting synchrotron magnets.

II. Magnet Programme

The superconducting pulsed magnets of relevance to a synchrotron programme, which have been completed and tested, which are being built and which are under design in the Karlsruhe IEKP Magnet Group are listed in Table I. After the two first stage magnets D1 and DT have been tested providing a lot of engineering and experimental experience, the prototype magnets D2 and D3 are fixed to produce a 4.5 T central field in an 8 cm aperture by a modified $\cos\theta$ current distribution, the coils being surrounded by a cold laminated iron yoke. The variability of the concept is demonstrated by the fact, that two different iron yokes (close saturated (a) and far unsaturated iron (b)) and two different conductor configurations (five double layers of a nearly square cable, two or three double layers of flat cable) will be used for dipoles D2a and D2b.

Adopting the version which proves to be best with respect to engineering considerations, meeting the design specifications and reliability, dipole D3 will be built with the only essential change of doubling the length, its geometrical dimensions being close to the requirements of a superconducting synchrotron concept.

The programme summarized in Table I reflects evidently the conductor development. Dipole D1 was wound from a multifilament superconducting wire, before the cabling and braiding technique necessary for high current conductors had been developed for commercial use. Dipole DT and D2a are wound from a InSn-soldered cable to avoid the undesirable training effect caused by wire movement. However, one has to put up with a severe disadvantage: the solder short circuits the individual strands and thereby increases the losses due to matrix currents. Thus, soldered cable magnets, from the point of view of tolerable ac losses, are only acceptable for field rise times of about 5 seconds or more. - Increasing the interwire resistivity by poisoning the solder and thereby reducing the losses has been studied by the BNL-Group.[1]

In the next stage dipoles D2b and D3, a fully insulated cable or braid will be used. This conductor concept completely removes the disadvantage of enlarged losses and thus enables shorter cycle times. To reduce - or even to avoid - training and degradation, the multistrand conductor should be impregnated with a filled epoxy resin system. In dipoles D2 and D3 the spacers, made from fibreglass reinforced epoxy, serve as compact filler, thereby only a small amount of resin will be needed.

Dipole D1. In a first stage a single multifilamentary superconducting wire was used to wind a dipole magnet of 0.5 m overall length (Fig. 1). The concept of intersecting ellipses was approximated by a computer programme to give a total calculated field error of 2×10^{-4}.

The magnet consists of 7 potted pancakes per pole with geometrical tolerances of $\pm$ 20 µm. The magnet exhibited training during the first 10 quenches to reach nearly its final dc field of 3 T at 45 A, which is about 30% of the short sample current at $\varrho = 10^{-13}$ Ωcm wire resistivity. Further cooldowns brought no significant improvement; probably coil movement has caused the degradation. In quench case the stored energy was nearly completely released in the magnet due to its high resistance in the normal state. The quench voltages per pole were about 500 V arising in 0.6 s, the current being reduced to 55% of the quench current.

Dipole DT. This magnet shown in Fig. 2 has been wound from a 10 strand cable with a central

[+]Work performed with the financial support of the "Bundesministerium für Bildung und Wissenschaft", Bonn.

TABLE I. IEKP Magnet Parameters

Magnet	D1	DT	D2a	D2b	D3
Magnet Parameters					
Coil aperture diameter or dimensions, inside of windings (mm)	110 x 80	80 x 40	80	80	80
Length (iron) (m)	0.5	0.4	1.4	1.4	2.8
dc field achieved (T)	3	4.5			
Pulse field achieved (T) at field rise time (s)	3 30	3.2 5			
Specified pulse field (T) at field rise time (s)			4.5 10 - 20	4.5 5 - 10	4.5 3 - 10
Operating current (A)	45	1035	1500		
Stored energy at 4.5T (kJ)	27 (at 3T)	15	(a)128; (b)142		
Iron shield inner diameter or dimensions (mm)	no	250 x 40 window frame	laminated iron yoke at helium temperature (a)172; (b)216		
Iron shield outer dimensions, cross section x length (m)		0.37x0.58x0.40	(a)0.3x0.38xl.4; (b)0.3x0.46xl.4		0.3x ? x2.8
Coil cooling	channels, bath cooling	channels, bath cooling	channels bath cooling, forced convection		
Coil and conductor					
Coil design	mod. intersect. ellipse, ends at 90°, potted	flat race track unpotted/race track ends at 45°, potted	modified cosθ, potted		
Number of layers/pole	-	34 } total coil	5 double l.	2-3 double l.	2-3 double l.
Number of turns /pole	5600	306 }	210		
Inductivity at 4.5T (mHy)	27000 at 3T	50	(a)130; (b)125		
Conductor manufacturer	VAC, Hanau, Germany	IMI, Birmingham, England			
Conductor type	multifilament wire	cable with central copper core, InSn-soldered		flat cable or braid with strands fully insulated	
Dimensions (mm)		1.9 x 2,64	2.1 x 2.6		
Cable insulation		glass braid	terylene glass br.		
Number of strands	1	10	12		
Strand diameter (mm)	0.4	0.5	0.54		
Transposition pitch (mm)	-	30	30.4		
Filaments per strand	130	1045	1000		
Filament diameter (μm)	25	10	12	8 - 10	8 - 10
Twist pitch (mm)	4	12.5	4	≤ 3	≤ 3
Matrix	Cu	CuNi	Cu		
Matrix: NbTi	1.2 : 1	1.5 : 1	1 : 1		
Max. current dens. at 4.5T			(a) (b)	Conductor not yet finally fixed	
superconductor	79 } at 3T	130	117 129		
strand (kA/cm²)	36 }	53	59 65		
cable	-	21	25 27		

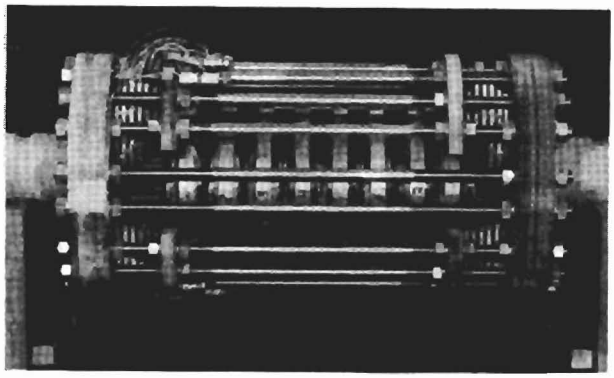

Fig. 1 Dipole D1.

copper core, the cable being InSn-soldered to ensure mechanical rigidity. The cold laminated iron yoke is of the window frame type with the rectangular window widened in a hyperbolic shape towards the ends providing for a linear field decrease. The 1 mm iron sheets are insulated by a 7 µm phosphate coating and screwed together by means of 4 epoxy insulated stainless steel pins passing through the outer parts of the yoke. The coils were fixed within the window by means of wedges. The cable was wound to an unpotted flat race track coil in the first test stage. Cooling channels were spaced 4.5 mm from each other (every two layers). The magnet was mounted vertically and has been operated under bath cooling conditions. After precooling to $1N_2$ temperature, 0.15 liter helium per kg iron were necessary for the cool down.

During the first period of operation, the magnet has been tested for almost 10000 cycles with triangular pulses of 2, 5 and 10 seconds pulse duration. At a slow field rise of ~ 0.1 T/s, a central field of 4.5 T and a peak field of 5.2 T on the winding surface were obtained with a magnet current of 1035 A which is in accordance with the guaranteed short sample values. Neither degradation nor training was observed.

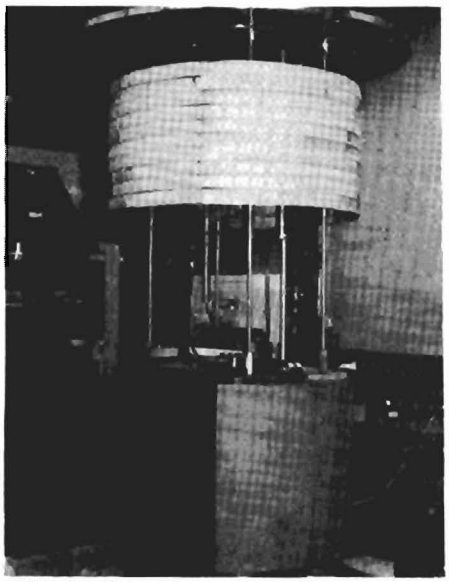

Fig. 2 Dipole DT.

The current field characteristics of the magnet are shown in Fig. 3. The calculated curves lie somewhat higher, which is due to an incorrect set of iron-µ-values in the computer programme input data, as has been shown by recent low temperature magnetization measurements of the iron used in DT; a recalculation will be done. In Fig. 3, two field curves of the coil without the iron yoke are included. Field measurements were taken with Hall probes and during field rise with an integrating fluxmeter.

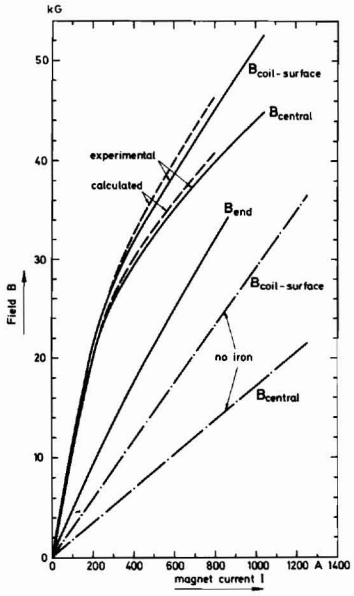

Fig. 3 Field vs current for dipole DT at the centre (x = y = s = 0), near the coil surface (x = 1.75 cm, y = s = 0) and at the end (x = y = 0, s = 20 cm).

For the case of quenching the coils were protected by a comparator device, which inverts the power supply mode to an energy feed-back mode, if there is an ohmic resistance in the coil corresponding to a voltage drop of ~ 1 V. The comparator consisted of a copper coil, which was adjusted to give the same induction voltage as did the superconducting coil. The maximum current could be decoupled from the coil in about 1 second. Even in the worst case of the coil being totally in the normal state, its time constant L/R (L = 150 mHy for unsaturated iron, L $\simeq$ 50 mHy at 4.5 T with saturated iron) is at least one second, thus nearly the total stored energy could be removed from coil. The decoupling device worked perfectly, the coil could be quenched without observing an increase in the boil-off rate.

Losses were determined by measuring the He boil-off rate and later by a Hall multiplicator device. Results are shown in Fig. 4 and Table II.

TABLE II. Losses in Dipole DT at Peak Field

Rise Time (s)	Peak Central Field ("Permanent Pulse Mode") (T)	Losses (J/cycle)
45	4.5	<8
31	3.5	14
5	3.2	130
2.5	3.0	107
1	2.4	90

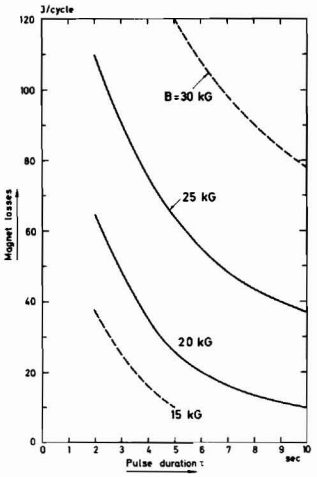

Fig. 4 Losses for dipole magnet DT vs. pulse duration for different central fields (triangular pulses).

The boil-off rate method is correct only within ~20% and rather time expensive to reach a stationary state. The peak field values given in Table II represent the maximum field attainable during half an hour pulsing ("permanent pulse mode"). Going to higher fields no stable permanent pulse operation could be achieved, although some few pulses could be run at higher fields without quenching the magnet. This peak field is reduced as the rise time decreases. The losses per cycle are approximately proportional to the frequency and the square of the field. This can be explained

- by the contribution of eddy current losses in the end region of the iron yoke (iron resistivity ratio = 8), where field components perpendicular to the laminates exist,
- by coupling losses, due to currents crossing the interwire solder resistivity layers and copper core (copper resistivity ratio = 140),
- possibly by shorts between adjacent layers. When the cable was wound off, the fibreglass tape insulation wrapped around the cable was found damaged at those points, where the coil was wedged in the magnet iron window.

It will be shown from the actual DT test runs with potted coils, whether shorts have made a considerable loss contribution. On the other hand, the severe influence of a low resistivity solder with respect to coupling losses is well known.[1] The high level of heat production in the coil is thought to be the reason for the lowering of the attainable field with increasing pulse frequency.- The iron hysteretic losses are about 8 J/cycle at maximum peak field, the superconductor hysteretic losses about 4 to 5 J/cycle, both being small compared to the frequency dependent losses mentioned before.

In a second test stage, the DT-cable is going to be rewound in two race track coils with ends bent at 45°, now being resin impregnated. Looking for possible training and measurements of attainable field and pulse losses are projected.

The same iron yoke has been used to build a magnet with coils wound from a high purity aluminum tape (8 x 0.3 mm cross section).[2] The tape is insulated by a 7 μm anodized coating which can stand annealing at 500°C. The coils were wound in a flat race track 60 cm long, the ends then being bent at 45° by press-working. The zero field short sample resistivity ratio of 9200+ could be recovered in the bent coils after annealing and subsequent epoxy impregnating to achieve mechanical rigidity. The magnet consists of 2 x 2 coils; one iron yoke half with coils and cooling channels is shown in Fig. 5.

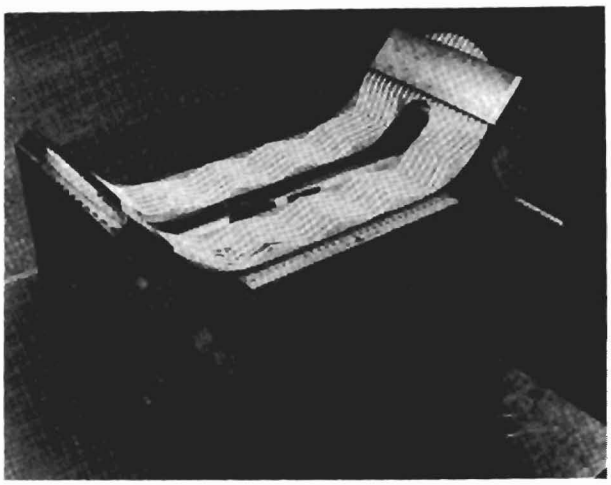

Fig. 5 Iron yoke of dipole DT with Al coils.

The total coil resistivity at 4.2 K vs. the magnet central field is given in Fig. 6 showing the magnetoresistance increase, which has been reported earlier.[4] The upper curve in Fig. 6 was taken in a later test run, where probably the mag-

+The conductor was produced and delivered by Vereinigte Aluminium-Werke (VAW), Bonn, Germany.[3] In the meantime, preparation has been improved to a 0.3 mm tape resistivity ratio of 15000 (allowing for size-effect correction).

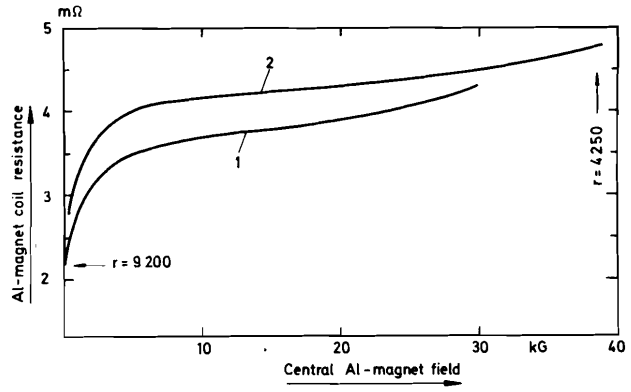

Fig. 6 Aluminium magnet coil resistance at 4.2 K vs magnet central field 1. at the first test run; 2. at a later test the resistance being increased probably due to coil deformation.

netic forces (~ 20000 kg over the coil length) during the preceding pulse tests have deformed the coils slightly and thereby induced lattice defects resulting in a resistance increase. - Field and loss measurements at 4.2 K are summarized in Fig. 7. The discrepancy between calculated and measured field levels for a given magnet current

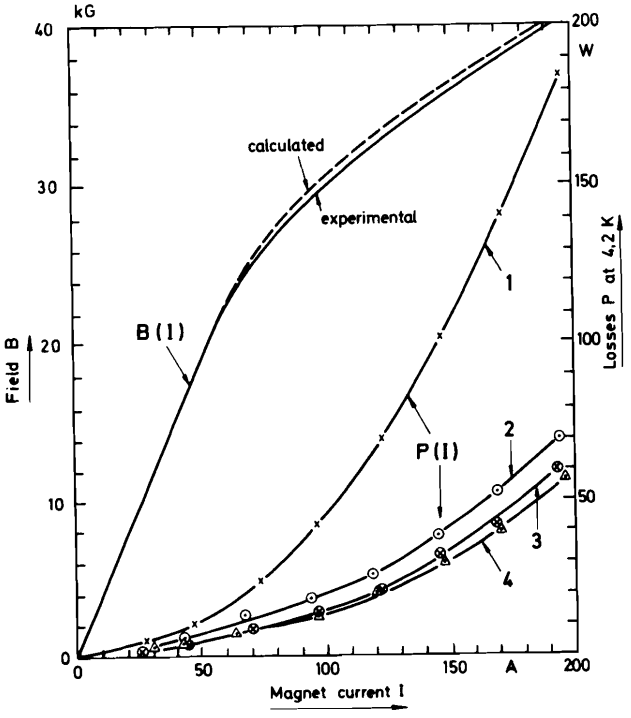

Fig. 7 Field B and losses P (triangular pulses) vs current for the aluminum magnet: 1. dc operation; 2. 3 sec, 3. 6 sec, 4. 10 sec pulse duration.

is again due to the incorrect μ-values as mentioned before. Losses have been determined electrically multiplying current and voltage by a Hall-generator device. In the triangular pulse mode operation they are about one third of those in dc operation as is to be expected; they are in fact somewhat lower, as when pulsing the mean resistivity is lower due to the magnetoresistance than the peak field resistivity responsible for the dc losses. The splitting of the loss curves for different pulse durations is caused by eddy current losses in the aluminium tape and iron and hysteretic losses in the iron.

Though losses in the range of 3 T and 5 seconds pulses are comparable for the superconducting and aluminium version of DT, probably potting the superconducting coils and especially using a fully insulated cable as in dipole D2b and D3 will show the superiority of the superconducting concept as to pulsed accelerator magnets with about 4 to 5 T peak field and pulse durations of 3 seconds or more.

Dipole D2a, D2b and D3. Dipole D2a, which is actually being wound, and dipole D2b and D3, which are under design, present various stages in the development of a superconducting synchrotron dipole. All three magnets will have coils which are based on the modified cosθ current distribution with an inner and outer diameter of 80 mm and 152 mm, respectively. The design induction for all is 4.5 T with a uniformity of 0.1% within a bore of 60 mm diameter; the multipole structure is described elsewhere.[5] The cosθ geometry permits one to build coils which are capable of generating uniform fields whether or not the iron shield is present.

Two iron yokes are being built presently.[+] One, which has an inner diameter of 172 mm, becomes saturated as the magnet goes to high induction; the other, which has an inner diameter of 216 mm, remains unsaturated throughout the cycle. The coils of D2a and D2b may be used in either iron shell (or with no iron at all). The effects of iron saturation on ac losses, field and field uniformity can be measured directly. The expected field as a function of current for both shells and no iron shell is shown in Fig. 9, the superconductor critical current as function of B and T being included. The expected iron enhancement of the field is given in Fig. 10.

The length of the iron shell for D2a and D2b is 1.4 m; the iron sheets are 1 mm thick with a 10 μm phosphate coating on each surface. The outside of the iron is shaped to counteract the effects of saturation. The ends of the magnet coil lie about 3 cm inside the laminations (Fig. 8) and are shaped to produce an integrated field which is good to 0.1%. The conductor positions shown in Fig. 8 are calculated by a computer programme in order to get the desired field homogeneity.

[+]Brown, Boveri & Cie, Mannheim, Germany.

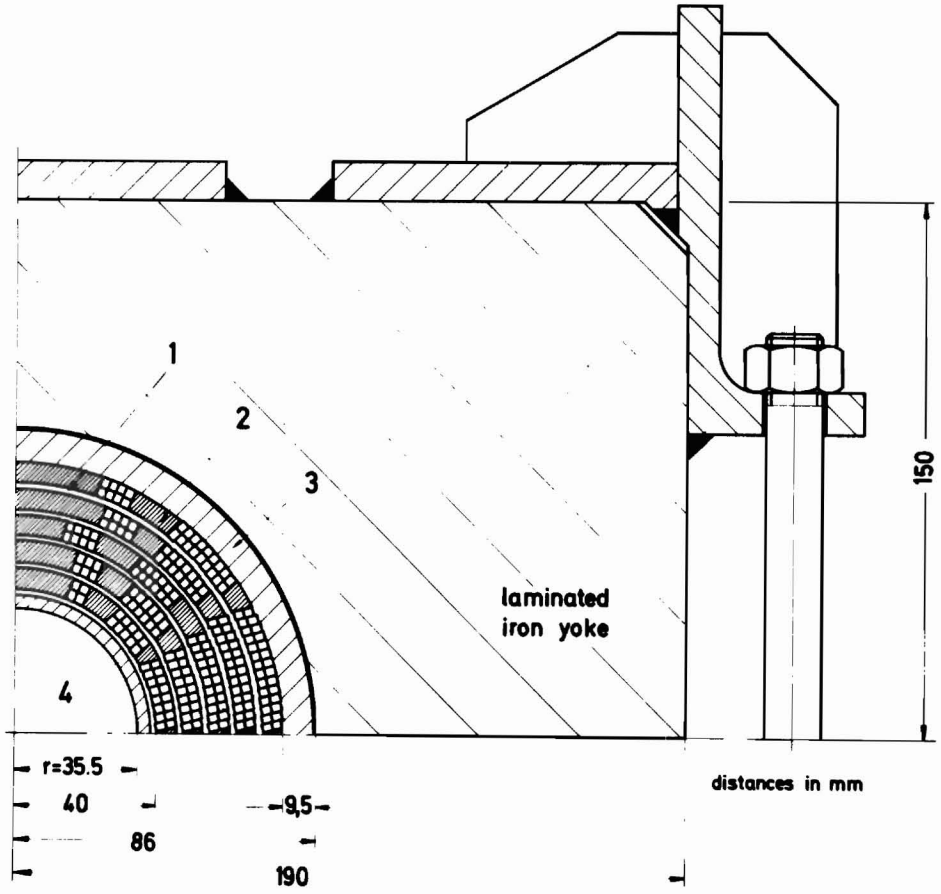

Fig. 8 Dipole D2a cross section with conductor configuration (left) and longitudinal section with conductor end configuration (below): 1. Cooling channels, 1.5 mm in width; 2. spacers, glass fibre reinforced epoxy; 3. support rings, stainl. steel; 4. tube, stainl. steel; 5. yoke top and end plate, stainl. steel; 6. sleeve, glass fibre reinforced epoxy; 7. guide pin; 8. Belleville springs; 9. Cooling hole; 10. front panel, stainl. steel.

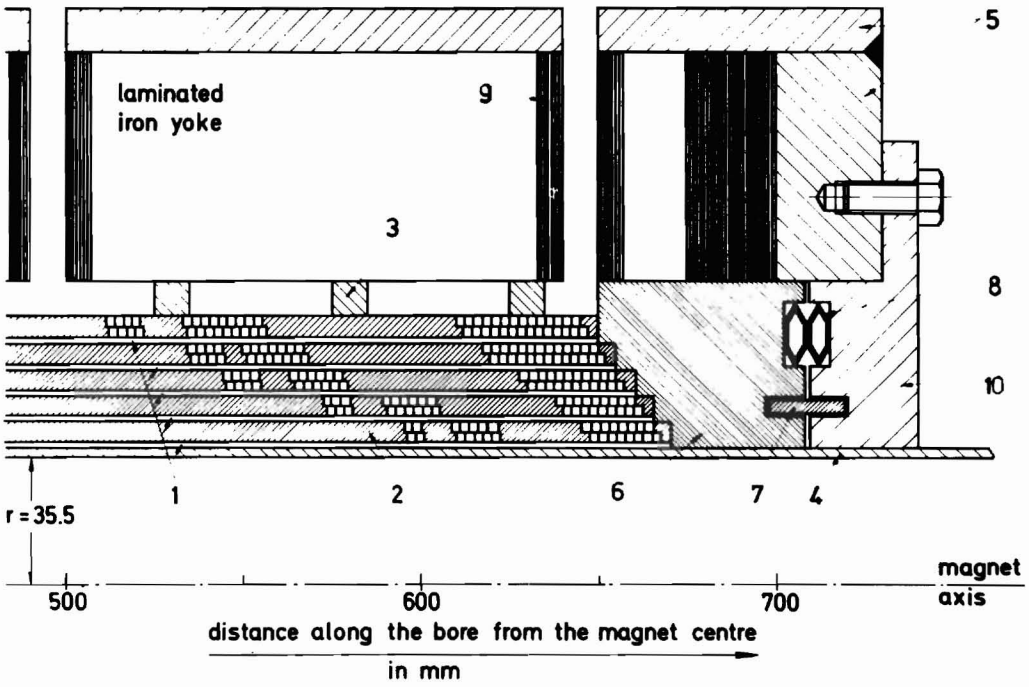

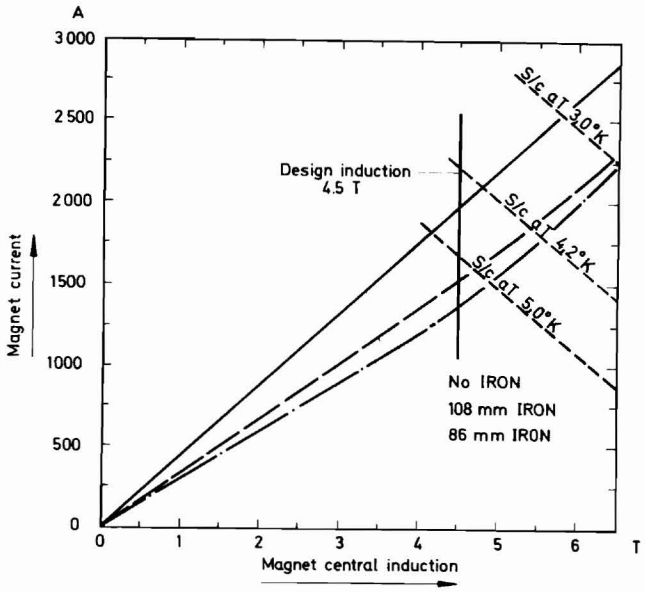

Fig. 9 Dipole D2a operating current vs central induction, calculated for the different iron versions. Guaranteed short sample values of superconducting cable.

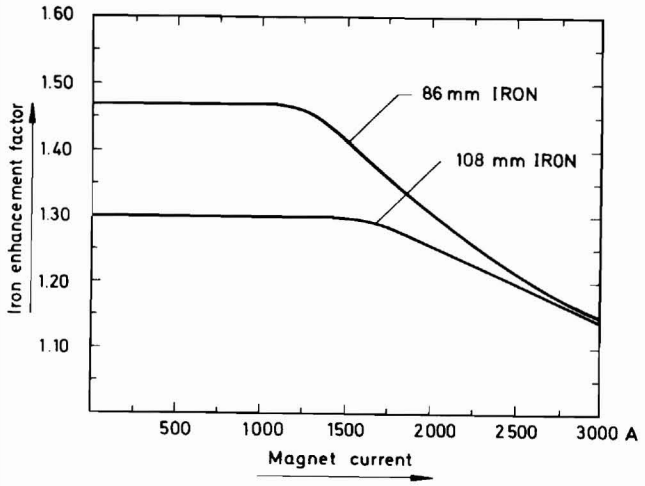

Fig. 10 Calculated iron enhancement factor for dipole D2a central induction; saturated and unsaturated version with 86 mm and 108 mm iron inner radius resp.

Since the radial dimensions of the coil package in all three dipoles are the same, many of the accessory parts such as bore tubes, force restraining fixtures and holding fixtures are identical. The coil design, on the other hand, is quite different for the three magnets. Dipole D2a has a 5 double layer coil which is fabricated from almost square conductor (Fig. 8). It requires 10 separate winding and potting operations and 10 pairs of electrical leads to be interconnected. Dipole D2b is greatly simplified by reducing the number of cable layers to 2 or 3 depending on the flat cable or braid superconductor, which is available at that time. Thereby dipole D2b will be easier to wind, pot and assemble than D2a. Dipole D3 will incorporate the same coil design as D2b except that the coil and iron length will be extended to 2.8 m.

The superconductor for dipole D2a is a soldered cable with 2.1 x 2.6 mm cross section;[+] it is wrapped with a terylene-glass braid insulation 0.2 mm thick. The 2.5 x 3 mm insulated conductor cross sections are shown in Fig. 8. A current of 2000 A at 5 T and 4.2 K has been guaranteed. It is expected that the maximum field in the conductor of D2a will be about 4% above the central field. Dipole D2b and D3 will use a flat cable or braid with fully insulated strands. Our preference is towards the cable, because crossover points which are potential shorts are eliminated. The cable has a packing factor of about 70% compared to the braid with about 50%. It is expected that dipole D3 will have a conductor similar to that of D2b.

Magnetic forces will be supported by stainless steel rings, the space left between the coil and the iron being filled with helium. Holes in the iron permit helium to flow from the bottom into the magnet, through the cooling channels of the coils and out of the magnet through the holes in the top of the iron. The cooling channels will also make possible forced cooling lengthwise through the coils. The largest dimension of both iron shells permits them to fit into a cylinder with a diameter of 590 mm. Two cryostats[++] have an inner vessel with a free space of 600 mm diameter by 1530 mm in length (see Fig. 11). The cryostats have a warm bore which is slightly larger than the 60 mm useful aperture. They are equipped with two 100 mm diameter necks, one for the refrigeration, the other for electrical leads and service valves. An outer vacuum jacket and a support system is being built, which can be modified for use with dipole D3. We intend to make the inner cryostat vessel of dipole D3 an integral part of the magnet itself.

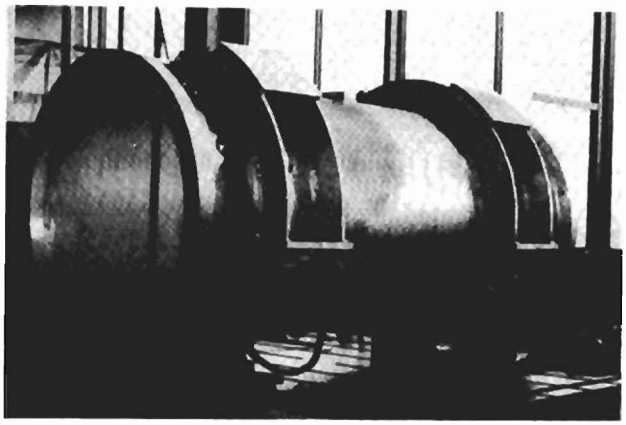

Fig. 11 Cryostat for D2a, D2b (outer vessel).

[+] IMI, Birmingham, England.

[++] Leybold-Heraus, Köln, Germany.

Refrigeration for the dipoles[6] will be supplied by the Karlsruhe 300 W Linde refrigerator and later by the 300 W refrigerator built by Messer Griesheim. Cold helium gas is delivered from the refrigerator to the magnet cryostat by a concentric transfer line system consisting of a rigid transfer line from the refrigerator to the magnet test area and three flexible transfer lines to the magnet cryostats.[7] The J-T-expansion takes place in the magnet cryostat.[+]

The pulsed dipole magnets are charged with a thyristor controlled power supply (BBC) capable of delivering 3500 A at 70 V in a ramp function. The voltage to do this is generated by a rectified three phase circuit which is thyristor controlled. The remaining 600 Hz ripple is reduced by different filters to a few parts in 10^4. The power supply can be used to extract the magnet stored energy during a quench. A superconducting solenoid is being built (4 T, 116 kJ; 8 T/s; split coil length: (2 x 15) + 1 cm, inner diameter: 15 cm; 24 strand IMI braid) for testing the power supply and the quench protection device. Field measurements of dipoles D2 and D3 will be taken by a moving bucking coil system with computer drive and data acquisition.

III. Conductor and Materials

Conductor Studies

One of the central problems of pulsed superconducting magnet work is the choice of a suitable composite superconductor. The many parameters which characterize a multifilament composite and a cable or braid made of them, should be optimized with respect to mechanical, thermal and electrical performance according to technical feasibility. One important feature to be optimized is the ac loss behaviour of superconducting composites,[8,9] which is reasonably well understood. On the other hand, the relation between short sample characteristics of multifilament composites and their behaviour as wire, braid or cable in an unpotted or potted coil or test magnet, i.e. degradation and training effects, still has to be studied more thoroughly.

Short Sample Measurements. A lot of multifilament NbTi wires with different filament diameters down to 4 μm has been examined. Their short sample characteristics were plotted as $\log \varrho = f(\log J)$, where the overall wire cross section is taken to determine the wire resistivity ϱ and the current density J. The steeper the slope of the characteristic, the more the multifilament wire approaches the behaviour of a single core conductor.[10]

When wound to a solenoid or magnet, the resistivity of the wire might cause degradation depending on cooling conditions. In order to have comparable cooling conditions in the short sample tests and in magnet operation, the short samples (~3.5 m long) were wound into a small bifilar multilayer coil potted with epoxy resin. Compared to a well cooled single wire loop sample (~15 cm) tested earlier, a considerable reduction in take-off current has been observed. Therefore we had to use single loop samples with the better cooling performance for resistivity above $\sim 10^{-11}$ Ω cm.

A selection of tested wires is given in Table III. All samples have a twist pitch of a few millimeters. Conductor (c), (d) and (e) were taken from braids or cables.

TABLE III. Parameters of some Tested Wires

Conductor	Wire Diameter (mm)	Filament Diameter (μm)	Number of Filaments	Cu:Sc Ratio
(a)	0.4	10	300	3.8 :1
(b)	0.4	24	130	1.2 :1
(c)	0.28	10	361	1.25:1
(d)	0.38	8.5	1000	1 :1
(e)	0.2	7.5	400	1 :1

Conductor (a) was known to be mechanically defective and showed many broken filaments after the copper matrix had been carefully etched away. The characteristics for (a) have a small slope of about $1.5 = \log\varrho/\log J$ nearly constant for the field range from 1 to 4.4 T. The steepest slope of about 50 has been observed for the two conductors (c) and (d). Their characteristics are so close together, that only the curve for (d), together with (b) and (e), is shown in Fig. 12. In this diagram the upper points give the take-off current. The lowest measured resistivity was 3×10^{-14} Ω cm at low fields. Microscope photographs of composite cross sections show that the filament diameter for conductor (c) is nearly constant, whereas filaments in (d) and even more in (e) vary considerably in size; in (b) several filaments are connected together.

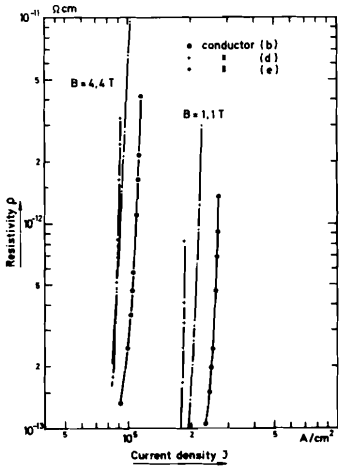

Fig. 12 Resistivity ϱ vs current density J for conductors (b), (d) and (e) wound in bifilar coils.

[+]Manufacturers involved: rigid transfer line: Leybold-Heräus; flexible transfer line: Vacuum Barrier; J-T-expansion including controls: Linde.

Systematically more samples have to be studied, before a satisfactory explanation can be given, how the wire parameters will affect the short sample characteristic.

Test coils. Different NbTi multifilament wires were wound to 35 cm long test coils cast in epoxy resin with ends bent at 90°. These coils are similar to the race track coils in dipole D1.

Looking for training effects, it could be shown that thermal cycling before the electrical tests reduced the training. Once the coil had been trained, the quench currents were constant within 0.1% for some coils and no more affected by thermal cycles. The dc quench currents had to be related to resistivity values less than 10^{-12} Ω cm, neglecting the other effects which could cause degradation as one has to assume in the dipole magnet.

The development of conductors for pulsed superconducting synchrotron magnets tends to use high current ac cables or braids to restrict charging voltages to reasonable levels. Two insulated braids of rectangular shape, the first consisting of 48 strands of conductor (c), the second of 24 strands of conductor (d) were wound to small unpotted test solenoids of 6 cm length and 4 cm inner diameter with cooling channels between every two layers. The load lines of these solenoids are shown in Fig. 13. To find the short sample curves, the averaged single strand values of the (c)- and (d)-wire at a resistivity of 10^{-13} Ω cm have been multiplied by the number of strands. Testing the solenoid wound from braided conductor (d), one end of the braid outside the magnet burned out during pulsing the solenoid with a frequency of 2 Hz. The braid end was mechanically unsufficiently fixed, which might have caused strand breakage during pulse operation. After repairing the braid end, the solenoid went to a 10% higher quench current as is shown in Fig. 13 on the load line.

The solenoids which will be tested next will be potted, including also soldered braids and cables.

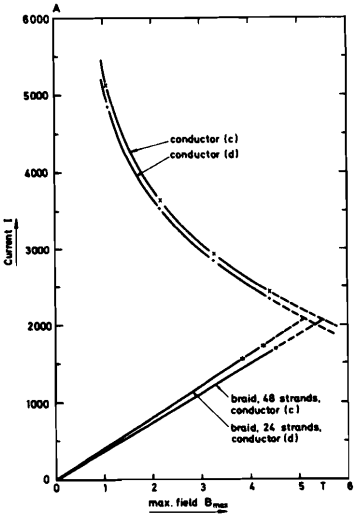

Fig. 13 Short sample curves and load line for unpotted test solenoids of 48 strand braid (conductor (c)) and 24 strand braid (conductor (d)).

Low Temperature Material Studies

To determine the low temperature mechanical, thermal and electrical properties of materials used in magnet engineering, an extensive test programme has been started. Work was concentrated first on studying organic structural materials since generally no comprehensive data are available in this field.

Thermal contraction has been measured for different types of epoxy resins.[11] Inorganic fillers (quartz, Al_2O_3) of various grain sizes have been used. The contraction can be reduced considerably by loading the resin to match the contraction coefficients of metals. With fibre glass as filler contraction of resins can in addition be varied by the angle of the filament structure to the direction of contraction considered, as has been shown earlier.[12]

Thermal conductivity measurements of different epoxy resins and superconducting coil windings between 4 K and 10 K have been performed.[13] By admixture of Al_2O_3-powder the thermal conductivity of the resin could be considerably improved (CIBA CY 221/HY 956). Thermal conductivity of coil windings in the coil axis direction could be enlarged by a factor of ~4 by choosing a superconducting wire with a copper matrix and, at the same time, potting the coil with Al_2O_3-filled resin, compared to a CuNi-matrix wire potted with an unfilled resin. - Further measurements of filled and unfilled resins are being performed.

To investigate the mechanical behaviour of materials from 4.2 K to 300 K, a servo-hydraulic testing machine will be ready for operation by the end of 1972. A similar apparatus which operates down to $1N_2$ temperature has been installed in the "Institut für Kunststoffprüfung" of the University Stuttgart. Measurements of the Young and shear modulus and the Poisson ratio of rigid and flexible resins, unfilled and filled, with variable defor-

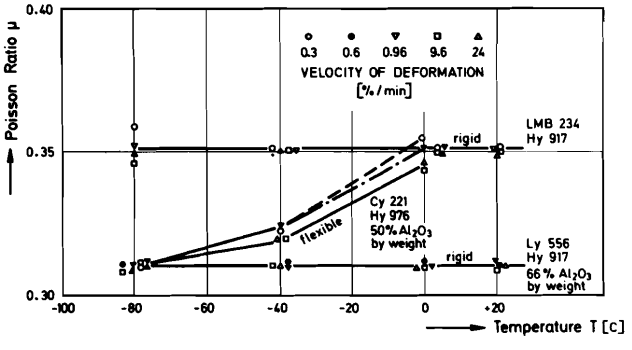

Fig. 14 Poisson ratio for different epoxy resin systems vs temperature.

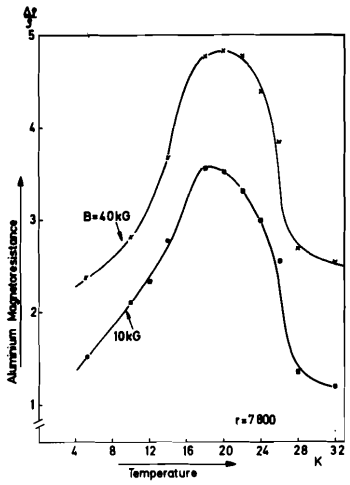

Fig. 15 Transverse magnetoresistance of aluminium tape (8 x 0.3 mm cross section) vs temperature. B = 1 T, 4 T parallel to the 8 mm side; residual resistivity ratio r = 7800.

mation velocity have been performed. The Poisson ratio vs temperature for three systems is shown in Fig. 14. A decrease as the temperature is lowered has only been observed for the system, which is flexible at room temperature. - To study crack formation in the resins, a corona test apparaatus[14,15] is being built.

Resistivity and magnetoresistance behaviour of aluminium tape conductor has been examined.[16] Short sample transverse magnetoresistance with the field parallel to the long side of the tape cross section has been measured in a sc solenoid in dependence of purity (given by the residual resistivity ratio r) and temperature with regard to magnet application. - As an example, results of $\Delta\rho/\rho = (\rho(B,T) - \rho(0,T))/\rho(0,T)$ vs temperature for 1 T and 4 T field and r = 7800 are given in Fig. 15.

Irradiation Tests

To study the nuclear irradiation influence on the properties of superconductor and structural materials, an experimental setup for low temperature irradiation measurements has been built.[17] It uses the Karlsruhe isochronous cyclotron as radiation source with 25 MeV protons, 50 MeV deuterons and 100 MeV α-particles. The probes are irradiated at 1He temperature and measured at 4.2 K in the same bath. The cryostat is equipped with a sc solenoid (6 T; 95 mm i.d.) for magnetic measurements.

An apparatus for magnetization measurements of superconductors has been built for the irradiation setup. Magnetization and hysteretic loss measurements for unirradiated samples of NbTi, NbZr, V_3Ga, Nb_3Sn have been performed.[18]

The irradiation apparatus did run several calibration tests for making the possible range of experimental conditions with a maximum of 2 μA deuteron and 1.5 μA α-particle current. Irradiation dose and dynamic He-loss measurements with a NbTi 130 filament conductor have been performed. For 100 MeV α- particle irradiation liquid helium losses of about 50 liters per μAh have reached the capacity limit of the recently installed helium gas recovery system. The temperature rise of the probe under investigation in the beam spot center can be measured by the calibrated resistivity-temperature dependence beyond the transition temperature.

Room temperature studies on stabilized NbTi multicore wires with 51.5 MeV deuterons up to doses of $\sim 10^{11}$ rads have been performed.[19,20] The critical current decreased by $\sim 25\%$ at 10^{11} rads (with no recovery) and by $\sim 10\%$ for lower dose rates of 10^{10} rads (with complete recovery). In the resistive state the power dissipated below take off is decreased by $\sim 20\%$ after 4×10^{10} rads irradiation.

References

1. A. van Steenbergen, editor, "Progress Report on Magnet Development, Brookhaven Nat. Laboratory," Proc. 8th Int. Conf. on High Energy Accelerators, CERN, Geneva, p. 199.
2. B. Lott, W. Schauer, W. Specking, S. Stumpf, P. Turowski, Technical Report Karlsruhe KFK (1972, to be published).
3. W.D. Hannibal, H. Pfundt, G. Winkhaus, Proc. 3rd Int. Conf. Magn. Techn., Hamburg, 1970, p. 1234.
4. W. Schauer, W. Specking, P. Turowski, Proc. 3rd Int. Conf. Magn. Techn., Hamburg, 1970, p. 606.
5. H. Brechna, M.A. Green, 1972 Applied Superconductivity Conf. Annapolis, Maryland-USA, 1972, p. 226.
6. H. Brechna, M.A. Green, W. Heinz, Proc. 8th Int. Conf. on High-Energy Accelerators, CERN-Geneva, 1971, p. 183.
7. W. Barth et al., 4th Int. Cryog. Eng. Conf. (ICEC 4), Eindhoven-The Netherlands, 1972.
8. K.P. Jüngst, G. Krafft, G. Ries, Technical Report Karlsruhe KFK 1217 (1970).
9. G. Ries, H. Brechna, Technical Report Karlsruhe KFK 1372 (1972).
10. F. Voelker, Part. Acc. 1, 205 (1970).
11. W. Weiss, Diplomarbeit Karlsruhe (1972).
12. H. Brechna, G. Hartwig, W. Schauer, Proc. 8th Int. Conf. on High-Energy Accelerators, CERN-Geneva, 1971, p. 218, and: Technical Report Karlsruhe KFK 1470 (1972).
13. G. Krafft, Technical Report Karlsruhe KFK 1347 (1971).
14. H. Brechna, E. Oster, Proc. Int. Sym. on Magnet Techn., SLAC-Stanford, 1965, p.313.
15. E. Schühlein, ETZ-A 80, 777 (1959).
16. B. Krevet, Diplomarbeit Karlsruhe (1972).
17. H. Becker, H.K. Katheder, E. Seibt, S. Steinacker, Technical Report Karlsruhe KFK 1684 (1972), and: S. Steinacker, Diplomarbeit Karlsruhe (1973).
18. K.R. Krebs, J. Pytlik, E. Seibt, Technical Report Karlsruhe KFK 1683 (1972), and: K.R. Krebs, Diplomarbeit Karlsruhe (1972).
19. H. Brechna, W. Maurer, Proc. 8th Int. Conf. on High-Energy Accelerators, CERN-Geneva, 1972, p. 224, and: Technical Report Karlsruhe KFK 1468 (1971).
20. W. Maurer, H. Brechna, Technical Report Karlsruhe KFK 1469 (1972).